Journal of Applied Electrochemistry **34**: 1287–1291, 2004.
© 2004 Kluwer Academic Publishers. Printed in the Netherlands.

Low-temperature SOFCs using biomass-produced gases as fuels

YANHONG YIN, WEI ZHU, CHANGRONG XIA*, CEN GAO and GUANGYAO MENG
Laboratory of Biomass Clean Energy, Department of Materials Science and Engineering, University of Science and Technology of China, Hefei, Anhui, 230026 PR China
*(*author for correspondence, fax: +86-551-3606689, e-mail: xiacr@ustc.edu.cn)*

Received 31 March 2004; accepted in revised form 16 July 2004

Key words: biomass, biomass-produced gases (BPG), doped ceria, electromotive force, solid oxide fuel cells

Abstract

The electromotive force (e.m.f) is calculated for solid oxide fuel cells (SOFCs) based on doped ceria electrolytes using biomass-produced gases (BPG, 14.7% CO, 14.2% CO_2, 15.3% H_2, 4.2% CH_4, and 51% N_2) as fuels and air as oxidant. It reveals that the BPG derived e.m.f. is very close to hydrogen when doped ceria is used as the electrolyte. A 35-μm-thick samaria-doped ceria based single cell was tested between 450 and 650 °C using BPG as fuel. Maximum power density of about 700 mW cm^{-2} was achieved at 650 °C. The open-circuit voltage at 450 °C was 0.96 V, close to the calculated value. However, the cell power density using BPG as fuel was relatively lower than that using humidified hydrogen (3% H_2O), and close to that using humidified methane (3% H_2O). Impedance measurements indicate that the relatively lower power output may be attributed to the high anode–electrolyte interfacial polarization resistance when BPG is used as fuel.

1. Introduction

Solid oxide fuel cells (SOFCs) are currently attracting interest because of their advantages in terms of efficiency and fuel flexibility over other fuel cell types. SOFCs operated above 800 °C are often termed high-temperature SOFCs, and usually use yttria-stabilized zirconia (YSZ) as electrolytes. Those operated below 800 °C are called intermediate-temperature SOFCs. Low-temperature SOFCs are those based on thin film electrolytes of doped ceria and operated below 650 °C, sometimes, as low as 500 °C. Compared with the former two, low-temperature SOFCs have advantages such as shorter start time and using low-temperature durable metals for interconnect, heat exchangers, and other structure components.

It is widely accepted that SOFCs are flexible in the choice of fuels such as natural gas, methane, propane, butane, etc. [1–4]. SOFCs can also tolerate carbon monoxide and other impurities in the fuel. It is generally accepted that using hydrocarbon fuels will make SOFCs more flexible and efficient than other fuel cell variants.

Biomass is one potential source of renewable energy and has always been a major source of energy for mankind. Through thermochemical, chemical and/or biochemical processes, biomass can be converted into convenient solid, liquid, and gaseous fuels to meet a variety of energy needs. Biomass-produced gas (BPG) comes from gasification, pyrolysis, or anaerobic digestion of biomass. It is a complex and variable mixture of nitrogen, hydrogen, methane, carbon dioxide, carbon monoxide and other gases [5]. Similar to biogas, whose composition usually lies within the following ranges [6]: CH_4 50–70%, CO_2 25–50%, H_2 1–5%, N_2 0.3–3%, BPG is limited in certain applications because of its variability of composition [7, 8]. In addition, BPG cannot normally be used in combustion engine generators because of its low heat of combustion and poor ignition qualities, whereas electrochemical oxidation proceeds well for BPG. Therefore, it can be considered as a possible fuel for SOFCs. It has been shown that gases with composition similar to BPG such as biogas can produce significant power with SOFCs running at intermediate temperature. Staniforth et al. demonstrated that, with SOFCs biogas could provide power equivalent to hydrogen, even when the methane content was below the value at which normal combustion could occur. The power output varied with methane content, with maximum power production occurring at 45% methane [8, 9]. However, no reports are currently available on BPG as fuel for SOFCs, especially low-temperature SOFCs.

In this paper, we calculate the electromotive force (e.m.f.) for SOFCs using BPG as fuels. SOFC is essentially an oxygen concentration cell where an e.m.f. is produced due to the electrochemical potential gradient of oxygen between anode and cathode of the cell. The open circuit voltage (OCV) determined by the e.m.f. is considered to be an important parameter of cell performance. We also demonstrate the feasibility of running low-temperature SOFCs using BPG as fuel with a single cell based on a doped ceria electrolyte. The gas (BPG) was produced by gasification of rice husk in a fluidized-bed reaction without inert additives. Its composition was CO (14.7%), CO_2 (14.2%), H_2 (15.3%), CH_4 (4.2%), and N_2 (51%) [10].

2. Theoretical

The e.m.f. of SOFCs using fluorite structure oxides as electrolytes is given as the following equation 1

$$E = \frac{RT}{F} \mathrm{Ln} \frac{P_{O_2}^{*1/4}}{P_{O_2}^{*1/4}} + \frac{P_{O_2}^{\prime 1/4}}{P_{O_2}^{*1/4}} \tag{1}$$

where F is the faradaic constant, R is the gas constant, T is the absolute temperature, P'_{O_2} and P''_{O_2} are the oxygen partial pressures at cathode and anode, respectively, and $P^*_{O_2}$ corresponds to an oxygen partial pressure at which the oxygen ion transference number of the electrolyte becomes 0.5.

The cathode is fed with air as typically practiced in a fuel cell, so P'_{O_2} is assumed to 0.21 atm. P''_{O_2}, the oxygen partial pressure in the complex chemical system of BPG, can be determined thermodynamically. The composition of a mixture at equilibrium is calculated by means of the so-called Gibbs free energy minimization method. The total Gibbs free energy, G, is expressed by

$$G = \sum_{1}^{k} n_i \mu_i \tag{2}$$

where n_i is the molars of species i, μ_i the partial molar Gibbs free energy, and k the species number. It is minimized with respect to n_i at constant temperature and pressure.

$$d(G_{\mathrm{system}})_{T,P} = 0 \tag{3}$$

There are many different algorithm to obtain a set of n_i that satisfies Eq(3). Here we used Lagrange's method of undetermined multipliers for the calculation. Base on the method we can construct an equation set to obtain n_i.

$$\begin{gathered} \mu_i + \sum_{1}^{m} \lambda_j a_{ji} = 0 \\ \sum_{1}^{m} a_{ji} n_i - b_j = 0 \\ (i = 1, 2, 3, \ldots, k) \\ (j = 1, 2, 3, \ldots, m) \end{gathered} \tag{4}$$

where a_{ji} is amount of the atomic species j in the chemical formula of species i, b_j the total molar of j in the system, λ_j the undetermined multiply and m the number of atomic species.

For the convenience of solving these equations, they are linearized by performing Taylor expansion. Newton iteration is then used to get solution between temperature of 450 and 900 °C. The total gas species supplied in anode were normalized to 1 mol in this calculation, which is carried out using the program developed with MATLAB® software in our laboratory.

3. Experimental procedures

A single cell with thin film SDC ($Ce_{0.8}Sm_{0.2}O_{1.9}$) as electrolyte was prepared using a dry press process [12, 13] with SDC + 65wt.% NiO as anode and SDC + 70wt.% $Sm_{0.5}Sr_{0.5}CoO_3$ (SSC) as cathode. The anode and electrolyte bi-layer was co-fired at 1350 °C in air for 5 h to densify the SDC film. Slurry consisting of SSC-SDC and an organic binder was then applied to the electrolyte using screen-printing, which was subsequently fired at 950 °C in air for 2 h to form a porous cathode. The single cell was sealed on an alumina tube with silver paste. When using hydrocarbon as fuel, carbon deposition on the anode can be a major problem for SOFCs operating at high temperature. The deposited carbon may block the channels for gas transport and consequently degrade the performance of the cell. However, carbon deposition can be restrained if the cell is operated at low temperature [1]. Therefore, electrochemical characterizations were performed at temperatures from 450 to 650 °C under ambient pressure. Fuel-cell performances were measured with a home-build SOFC test system [14]. BPG produced from gasification of rice husk in a fluidized-bed reactor without inert additives was used as fuel, and stationary air as oxidant. Humidified (3% H_2O) hydrogen and methane were also tested for comparison. The flow rate of fuel gas was about 40 ml/min. Ac impedance was measured at open cell circuit in the frequency range from 0.01 Hz to 100 kHz using a CHI600A electrochemistry analyzer. The microstructure of the cell was revealed with a scanning electron microscope (SEM, Hitachi X-650).

4. Results and discussion

$P^*_{O_2}$ in Equation 1 for doped ceria is determined from experimental results as shown in Equation 5 [15]:

$$P^*_{O_2}(\mathrm{atm}) = 1.25 \times 10^{12} \exp\left(\frac{-578\,\mathrm{kJ}}{RT\,\mathrm{mol}}\right) \tag{5}$$

The e.m.f.s of SOFC using mixed electronic–ionic conductor as electrolyte is calculated with Equation 1 and Equation 5. The result is shown in Figure 1. When using YSZ, a pure oxygen-ion conductor as electrolyte, the e.m.f.s at 450 °C is 1.053 and 1.184 V for BPG and hydrogen fueled cells, respectively. It is shown that the e.m.f. for a hydrogen fueled cell varies with temperature monotonically, while the e.m.f. for a BPG fueled cell

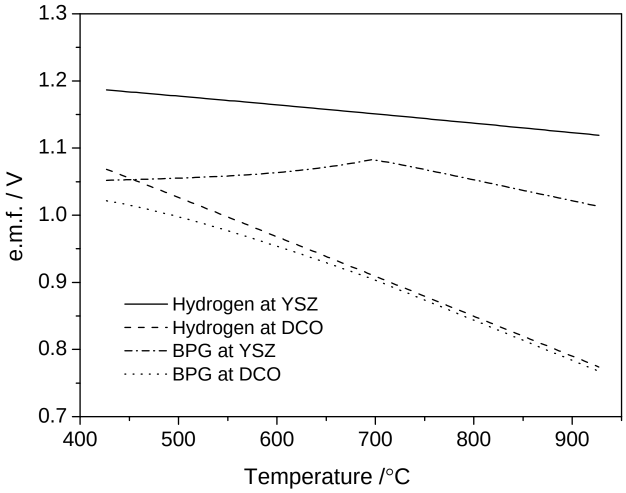

Fig. 1. E.m.f. as a function of temperature for SOFCs with yttria-stabilized zirconia (YSZ) and doped ceria (DCO) as electrolytes.

based on the YSZ electrolyte increases slightly from 1.052 to 1.083 V with temperature up to 700 °C and decreases rapidly to 1.021 V at 900 °C, which is due to the phenomenon of carbon deposition. At intermediate temperature the BPG derived e.m.f. is approximately 0.1 V lower than the hydrogen derived value. Figure 1 clearly shows that the e.m.f.s for SOFCs with doped ceria as electrolytes are lower than that with YSZ. The difference is due to the electronic conductivity of doped ceria. However, in a cell based on doped ceria the difference between the derived e.m.f.s for hydrogen and BPG is much smaller than that based on YSZ. Especially, the difference can almost be neglected at temperature above 650 °C.

Figure 2 displays the cross-sectional view of the cell after the testing. The SEM micrograph shows a 35-μm-thick dense SDC electrolyte sandwiched between the porous anode and cathode layers. No cross-membrane cracks or pinholes were revealed under SEM investigation. The anode and cathode are porous, and bonding strongly to the electrolyte.

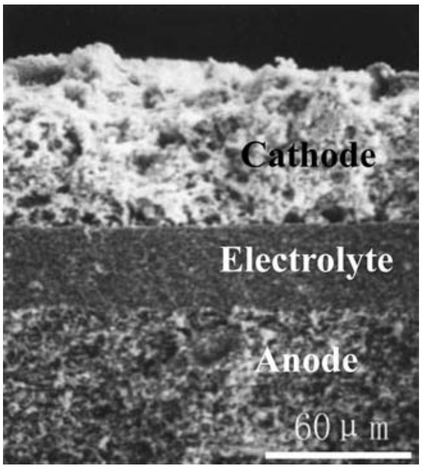

Fig. 2. SEM micrograph for the cross-sectional view of the single cell after testing.

The performance of the single cell was measured at temperatures between 450 and 650 °C using BPG as fuel. Figure 3 shows the cell voltage and power density as a function of current density. The open circuit voltage was 0.96 V at 450 °C, about 0.05 V lower than the calculated value as shown in Figure 1, and decreased to 0.95, 0.94, 0.90, and 0.86 V at 500, 550, 600, and 650 °C, respectively. The relatively lower OCVs might due to the thickness of the mixed conducting SDC, the thinner the electrolyte, the lower the OCVs [16]. It is reported that the OCVs across the cell with a thinner electrolyte (30 μm thick) were lower than those across the cell with a thicker electrolyte (0.4 mm thick) [17]. It is also possible that the gas flow rate contributes to the disagreement. The maximum power density is 700 mW/cm^2 at 650 °C, and decreases to 334 and 65 mW/cm^2 at 600 and 500 °C, respectively.

The long-term stability of the cell with BPG as fuel was performed at 600 °C. Results are shown in Figure 4. The voltage and current density changed as waves with

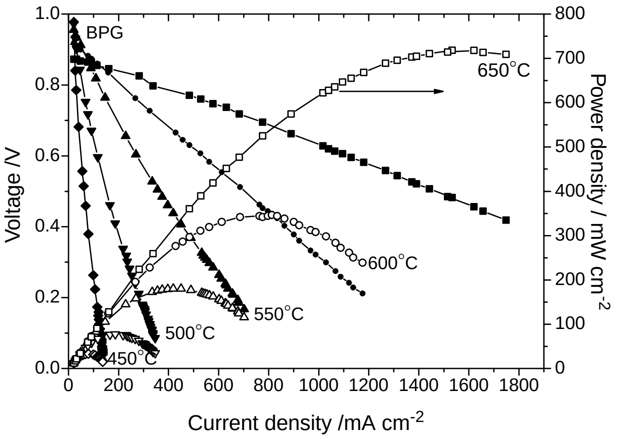

Fig. 3. Temperature dependence of cell voltages and power densities on current densities at 450–650 °C for the single cell with BPG as fuel and stationary air as oxidant.

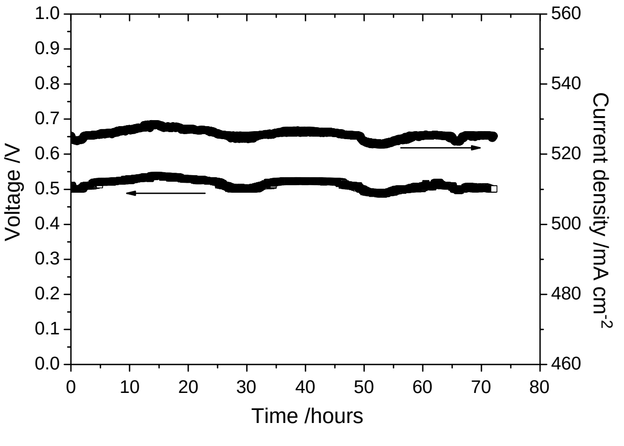

Fig. 4. Long term stability of the single cell operated at 600 °C with BPG as fuel.

time. The potential attenuation is 2% and ΔV (difference between the maximum and minimum potentials) is 0.05 V. And ΔI (difference between the maximum and minimum current densities) is 5.88 mA cm^2. No obvious performance degradation was observed inferring that carbon depositions are negligible during the time range considered in this work.

Humidified hydrogen and methane were also applied to the cell to compare the cell performances. When humidified hydrogen was used as fuel, power density is higher than that using BPG fuel. However, the power generated from BPG is close to that from humidified methane. Shown in Figure 5 are the cell voltage and power density as a function of current density for the same cell at 600 °C using humidified hydrogen, methane, and dry BPG as fuel. The OCVs derived from the three fuels are almost equal. This is consistent with the theoretical results as shown is Figure 1. Maximum power density at 600 °C is 491 mW/cm^2 derived from humidified H_2, 352 mW/cm^2 from humidified CH_4, and 334 mW/cm^2 from BPG.

The impedance spectra were measured at open cell circuit for the single cell using H_2, CH_4, and BPG as fuels. In these spectra, the diameter of the depressed semicircle corresponds to the interfacial polarization resistance of the anode and cathode. The total interfacial resistances for cell fueled with BPG are much larger than those with humidified hydrogen. Shown in Figure 6 is the spectra measured at 550 °C. The total area specific interfacial resistance for cell fueled with BPG is 0.38 Ω cm^2, much higher than those with humidified hydrogen (0.23 Ω cm^2), and methane (0.30 Ω cm^2). As the same single cell was used in impedance measurement and the conditions for the cathode were completely fixed, any difference by varying experimental conditions (except operational temperature) arose only from the change in the anode processes. It is demonstrated that the anode polarization resistance determines the high frequency arc, usually over 100 Hz [18]. As shown in Figure 6, area specific resistances corresponding to arcs lower than 100 Hz are almost the same, 0.15 Ω cm^2 for the cell with BPG, hydrogen, and methane as fuels, whereas the anode polarization resistance, corresponding to spectra at frequency higher than 100 Hz is much greater for BPG than that for humidified hydrogen fuel. So it can be deduced in the rough that at the same temperature, the anode interfacial resistance when using BPG as fuel is larger than that when using H_2, and CH_4, which indicates that anode polarization is one of the reasons that contribute to the relatively poor performance when using BPG as fuel. So it is desirable to develop highly catalytic active anode materials for SOFCs using BPG as fuels.

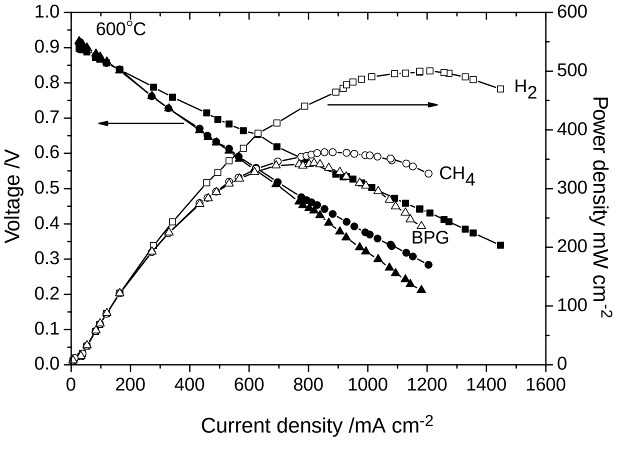

Fig. 5. Cell voltages and power densities as a function of current densities of the cell at 600 °C with BPG, humidified hydrogen (3% H_2O), and humidified methane (3% H_2O) as fuels.

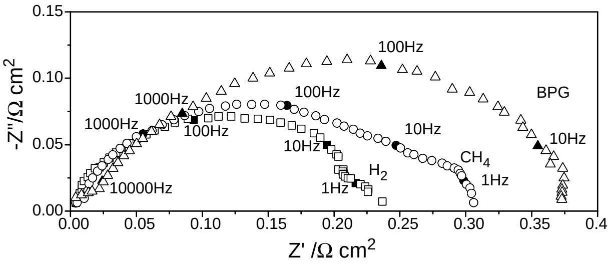

Fig. 6. Impedance spectra at 550 °C for the single cell with H_2, CH_4, and BPG as fuels.

4. Conclusions

The e.m.f. of SOFCs using BPG as fuels is calculated between 450 and 900 °C. The feasibility of using biomass-produced gas as fuel for low-temperature-SOFCs was demonstrated using a thin-film-SDC based fuel cell between 450 and 650 °C. Maximum power density is about 700 mW/cm^2 at 650 °C. It decreases with temperature, for example, to 334 mW/cm^2 at 600 °C. Maximum power density at 600 °C is 491 mW/cm^2 for humidified H_2, and 352 mW/cm^2 for humidified CH_4, respectively. However, the open cell voltages derived from the three fuels are almost the same. The relatively poor performance of the cell with BPG as fuel might be contributed to the high anodic interfacial polarization resistance. No performance degradation was detected inferring that carbon depositions are negligible during the time range considered in this work.

Acknowledgement

The work was supported by the National Nature Science Foundation of China under award NO.50372066 and 50332040.

References

1. E.P. Murray, T. Tsai and S.A. Barnett, Nature 400 (1999) 649.
2. S. Park, J.M. Vohs and R.J. Gorte, *Nature* **404** (2000) 265.
3. E.P. Murray, S.J. Harris and H.W. Jen, *J. Electrochem. Soc* **149** (2002) A1127.

4. Y. Jiang and A.V. Virkar, *J. Electrochem. Soc.* **148** (2001) A706.
5. A. Demirbas, *Energy Conver. Manage.* **42** (2001) 1357.
6. S. Bari, *Renewable Energy* **9** (1996) 1007.
7. J. Huang and R.J. Crookes, *Fuel* **77** (1998) 1793.
8. J. Staniforth and K. Kendall, *J. Power Sources* **71** (1998) 275.
9. J. Staniforth and R.M. Ormerod, *Catal. Lett.* **81** (2002) 19.
10. H. Jiang, X.F. Zhu, Q.X. Guo, Q.S. Zhu, *Indust. Eng. Chem. Res.* **42** (2003) 5745.
11. S.W. Zha, C.R. Xia and G.Y. Meng, *J. Appl. Electrochem.* **31** (2001) 93.
12. C.R. Xia and M.L. Liu, *Solid State Ionics* **144** (2001) 249.
13. C.R. Xia and M.L. Liu, *J. Am. Ceram. Soc.* **84** (2001) 1903–1905.
14. R.R. Peng, C.R. Xia, X.Q. Liu, D.K. Peng and G.Y. Meng, *Solid State Ionics* **152–153** (2002) 561.
15. T. Kudo and H. Obayashi, *J. Electrochem. Soc.* **123** (1976) 415.
16. M.L. Liu, Ionic and mixed conducting ceramics, *in*: T.A. Ramanarayanan, H.L. Tuller (Eds), '1st International Symposium, The Electrochemical Society' Vol. 91–12 (1991) pp. 191–209.
17. C.R. Xia, W. Rauch, F.L. Chen and M.L. Liu, *Solid State Ion.* **149** (2002) 11.
18. J.H. Koh, Y.S. Yoo, J.W. Park, H.C. Lim, *Solid State Ion.* **149** (2002) 157.